

## Liquid-Liquid Phase Transformation in Carbon

James N. Glosli and Francis H. Ree

*Lawrence Livermore National Laboratory, Livermore, California 94550*

(Received 7 October 1998)

A first order phase transition is found in liquid carbon using atomistic simulation methods and Brenner's bond order potential. The phase line is terminated by a critical point at 8801 K and 10.56 GPa and by a triple point on the graphite melting line at 5133 K and 1.88 GPa. The phase change is associated with density and structural changes. The low-density liquid is predominantly  $sp$  bonded with little  $sp^3$  character. The high-density liquid is mostly  $sp^3$  bonded with little  $sp$  character. This is the first nonempirical evidence of a liquid-liquid transition between thermodynamically stable fluids. [S0031-9007(99)08961-9]

PACS numbers: 61.20.Ja, 05.70.Fh, 64.60.-i, 64.70.Ja

Ferraz and March [1] suggested the existence of a liquid-liquid phase transition (LLPT) for the phase diagram of carbon in 1979. The first quantitative theory that explored the LLPT was a semiempirical equation of state modeling of carbon by van Thiel and Ree [2] in 1993. However, it was not until 1997 that the first experimental, though indirect, evidence for the LLPT in carbon was published [3]. This careful work on the melting of graphite by Togaya suggests that the slope of pressure-temperature ( $P$ - $T$ ) melting line is discontinuous at the temperature maximum, and hence at least three stable phases coexist at this point. The most likely conclusion is that this point is a triple point and the carbon phase diagram exhibits a LLPT.

Though somewhat exotic, LLPT's have been suggested in liquid S, Ga, Se, Te, I<sub>2</sub>, Cs, and Bi [4]. Recent experiments [5] and molecular dynamics (MD) calculations [6] have shown evidence of a first order transition between metastable phases of supercooled water.

The purpose of this Letter is to report the findings of a MD simulation of liquid carbon showing clear evidence of a LLPT. The LLPT line in carbon is mapped out, including the critical point at high  $T$  and the triple point at low  $T$ . The low-density liquid (LDL) phase has different local structure than the high-density liquid (HDL) phase. An order parameter sensitive to this local order change is defined and examined as a function of  $T$  and  $P$ . This is the first time that atomic simulations have directly observed a first order LLPT between two *distinct thermodynamically stable* liquid phases in carbon or any other material.

To describe the carbon-carbon interaction, the hydrocarbon potential model developed by Brenner [7] is used. The Brenner potential falls in a class of empirical potentials known as bond-order potentials having the simple form

$$\Psi = \sum_{ij \in \{\text{bonds}\}} \{\phi^R(r_{ij}) - b_{ij}\phi^A(r_{ij})\}, \quad (1)$$

where  $\phi^R$  and  $\phi^A$  are exponential functions representing the repulsive and attractive terms, respectively, in the bond energy. Although a sum over bond energies ( $\{\text{bonds}\}$  is the set of all bonds), this is not a pair potential. The so-called bond-order factor  $b_{ij}$  is a many-body factor and depends

on bond angles, torsional angles, bond lengths, and atomic coordination in the vicinity of the bond. This many-body nature of  $b_{ij}$  allows bond energy to depend on the local environment in such a way so as to produce the correct geometry and energy for many different carbon structures including graphite and diamond.

The simulations are performed mostly on 512 particle systems using a constant (cubic) volume ( $V$ ) and temperature MD. A number of calculations were done with 4096 particles to check for finite-size effects. The equations of motion are integrated using a velocity-Verlet algorithm [8] with temperature controlled via the N ose-Hoover thermostat [9]. To control integration errors, we have made the time-step variable by choosing it to be the lesser of  $10^{-15}$  sec or the time to ensure that the largest particle displacement is less than  $0.1 \text{ \AA}$ . In practice this results in 1200 to 2000 time steps per picosecond for  $T$  between 5500 and 9000 K.

The  $P$  isotherms are generated for  $T$  between 5500 and 9000 K at 500 K increments. Each isotherm is calculated at 61 volumes by varying the side of the computational box in  $0.1 \text{ \AA}$  increments from 14 to  $20 \text{ \AA}$ . The pressure is averaged over 1 ns of simulation. In total, this is about  $8 \times 10^8$  time steps or  $0.5 \mu\text{s}$  of simulation. To check for metastability or slow convergence, the volume is increased in small increments from  $(14 \text{ \AA})^3$  to  $(80 \text{ \AA})^3$  and then decreased back to  $(14 \text{ \AA})^3$ . For each volume the simulation was run for 1 ns. No hysteresis loop in the isotherms was observed within the statistical accuracy of the calculation. This is fairly strong evidence that the simulation is sufficiently long to sample all relevant phase space and is not being plagued by metastability.

The pressure isotherms are shown in Fig. 1. The classic van der Waals loop associated with a first order phase transformation is observed. The equal-area construction on the van der Waals loop is used to determine the phase coexistence region and the  $P$ - $T$  phase line, which are shown in Figs. 1 and 2, respectively. The numerical values are listed in Table I. The vanishing of the positive slope region of the isotherm with increasing  $T$  locates the critical point at 8802 K, 10.56 GPa, and  $8.70 \text{ \AA}^3/\text{atom}$ .

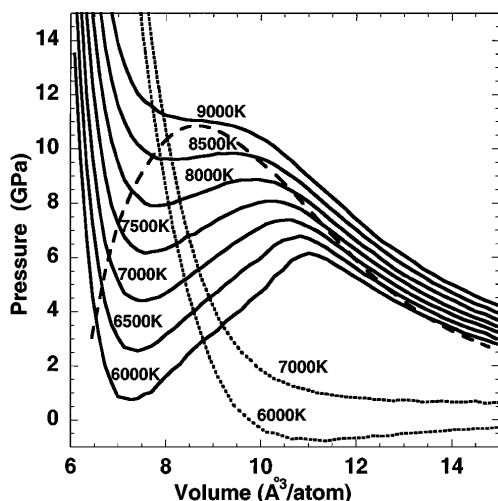


FIG. 1.  $P$ - $V$  isotherms are drawn as solid lines. The dashed line denotes the coexistence boundary. For comparison, the isotherms with torsion term removed are drawn as dotted lines. Error in the  $P$  is less than 0.05 GPa.

The dependence on system size was tested at 6000 K by increasing the number of particles, by a factor of 8, to 4096 particles. In the single-phase region the pressure and energy differences between the 512 and 4096 particle systems were less than 5% and 0.2%, respectively. In the coexistence region there was, as expected, significant changes with system size. The difference between the pressure maximum and minimum of the van der Waals loop decreased dramatically. However, the transition pressure and densities did not change significantly. In the 4096 particle systems the phase separation is easily observed in the coexistence region, further supporting the conclusion of a first order LLPT for molten carbon.

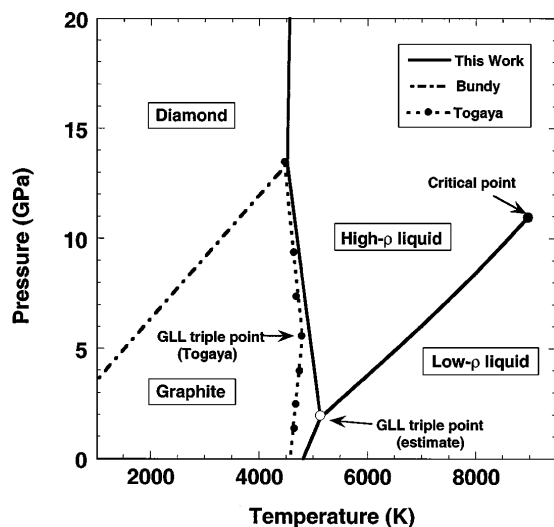


FIG. 2. Carbon phase diagram: dash-dotted line = experimental graphite-diamond line [11]; dashed line = experimental graphite melting line [2]; solid lines = simulation results using Brenner potential. The diamond melting line was calculated previously [10].

The locations of graphite-liquid-liquid (GLL) triple point and the graphite-melting line are estimated in the following way. At an initial guess for the GLL triple point, the volume and energy ( $E$ ) of graphite and both liquids are found by iterating  $V$  until obtaining the target  $P$ . At this point,  $dP/dT = \Delta S/\Delta V = (\Delta E/\Delta V + P)/T$  is evaluated, where  $\Delta S$ ,  $\Delta E$ , and  $\Delta V$  are the change of entropy, energy, and volume across the phase line. Under the assumption that the graphite-melting line has little curvature, which is consistent with experiment [2], the estimate of the triple point is improved by shifting the straight-line approximation for the graphite-melting curve to pass through the graphite-diamond-liquid triple point (4522 K, 13.42 GPa). This process can be iterated to improve the accuracy. In practice, the slopes change little from the initial estimate, and one iteration was sufficient. The initial guess for the triple point was at 5500 K and 2.69 GPa. For the liquid phases, see Table I for  $E$  and  $V$ . For graphite, a constant  $T$  and  $V$  simulation at 5500 K and  $7.644 \text{ \AA}^3/\text{atom}$  yielded  $P = 2.62 \pm 0.02$  GPa and  $E/N = 6.633 \pm 0.001$  eV/atom. Slopes of the graphite-HDL, graphite-LDL, and HDL-LDL lines are  $-0.0189$ ,  $0.00585$ , and  $0.00224$  GPa/K, respectively.

The results of these calculations are shown in Fig. 2. It clearly shows that the predicted LLPT lies within the *thermodynamically stable* fluid phase range. For reference, the diamond-melting line [10] based on the Brenner potential and Bundy's experimental results [11] for the graphite-diamond phase line and Togaya's experimentally determined graphite-melting line [2] are also shown. There is remarkably good agreement between Togaya's work and the present calculation, in particular, the slope of the high- $P$  part of the graphite-melting line. Togaya measured a value of  $-0.0258$  GPa/K and we estimate a slope of  $-0.0189$  GPa/K for the graphite-HDL phase line. This procedure locates the GLL triple point at 5133 K and 1.88 GPa. The experimental value is at  $4786 \pm 38$  K and 5.7 GPa. Although the temperature agrees well with experiment, the calculated pressure is small by a factor of 3. The underestimation of this pressure is not surprising and likely due to the absence of the longer-range van der Waals force in the Brenner potential. The net attractive nature of this force would stabilize the LDL phase to higher

TABLE I.  $T$ ,  $P$ ,  $V/N(\text{\AA}^3)$ , and  $E/N(\text{eV})$  for the HDL and LDL phases on the LLPT ( $\pm n$  denotes  $1-\sigma$  error in the last digit). The critical point temperature  $T_c = 8802 \pm 21$  K.

$T$ (K)	$P$ (GPa)	$V_{\text{HDL}}/N$	$V_{\text{LDL}}/N$	$-E_{\text{HDL}}/N$	$-E_{\text{LDL}}/N$
5500	$2.696 \pm 4$	$6.418 \pm 7$	$14.78 \pm 2$	$5.818 \pm 2$	$5.3202 \pm 7$
6000	$3.795 \pm 5$	$6.532 \pm 3$	$13.487 \pm 7$	$5.678 \pm 1$	$5.2477 \pm 4$
6500	$4.912 \pm 3$	$6.660 \pm 3$	$12.617 \pm 5$	$5.551 \pm 1$	$5.1686 \pm 3$
7000	$6.051 \pm 3$	$6.805 \pm 5$	$11.917 \pm 5$	$5.431 \pm 1$	$5.0875 \pm 3$
7500	$7.240 \pm 3$	$6.996 \pm 6$	$11.284 \pm 7$	$5.313 \pm 1$	$5.0071 \pm 3$
8000	$8.454 \pm 3$	$7.29 \pm 1$	$10.66 \pm 1$	$5.186 \pm 2$	$4.9329 \pm 3$
8500	$9.731 \pm 3$	$7.73 \pm 2$	$9.85 \pm 4$	$5.049 \pm 3$	$4.877 \pm 1$
8802	$10.56 \pm 6$	$8.70 \pm 3$	$8.70 \pm 3$	$4.906 \pm 4$	$4.906 \pm 4$

$P$ , in particular, at lower  $T$ , thereby reducing large density differences between the two fluid phases. Most likely, including a van der Waals term in the potential model would raise the calculated triple point pressure, decrease the slope of LLPT, and reduce the density difference between the HDL and LDL phases at the transition.

It is of interest to understand the structure of the two liquid phases. One measure of structure is the local coordination of each atom. For this discussion we use the same definition of coordination as used by Brenner [7]. This definition counts neighbors with weight 1 within 1.7 Å radius and with weight 0 outside a radius 2 Å. For neighbors with separation between 1.7 and 2 Å the weighting factor smoothly varies from 1 to 0 with separation. The present simulation shows that the coordination is highly correlated with the geometry of the local structure, and hence the hybridization state of the atom. Namely, the fourfold coordinated atoms are the centers of nearly tetrahedral structures, while the threefold coordinated atoms are the centers of planar structures with the neighbors at angles close to 120° and the twofold coordinated atoms tend to be linear. Therefore, twofold, threefold, and fourfold coordinated atoms will be  $sp$ ,  $sp^2$ , and  $sp^3$  hybridized, respectively.

Figure 3 shows “snapshots” of both the LDL and HDL phases at densities on the phase boundary. The color-coding highlights coordination and, as discussed above, the hybridization. Each configuration is from a simulation at 5500 K and 2.7 GPa. The LDL phase is dominated by chainlike  $sp$  structures with very little  $sp^3$  hybridized atoms, while the HDL phase contains mostly  $sp^3$  bonded atoms with very little  $sp$  hybridized atoms, similar to an amorphous “diamondlike” solid. Of course, both of these phases are liquids and the covalently bonded structures are continuously changing with time; however, the general character remains.

The order parameter,  $\Psi = (\rho_4 - \rho_2)/(\rho_4 + \rho_2)$ , where  $\rho_2$  and  $\rho_4$  are the number densities of twofold and fourfold coordinated atoms, is used to measure the local order. For instance, if  $\Psi = 1$  there is no twofold coordination, whereas for  $\Psi = -1$  there is no fourfold coordination. The order parameter is plotted in Fig. 4 as a function of pressure. The first order nature of the transition is clearly seen for  $T$  below the critical temperature ( $T_c$ ). For  $T \approx T_c$  the onset of the singular behavior associated with a second order transition is observed. Furthermore, although there is a significant number of threefold coordinated atoms in the coexistence region, a stable phase dominated by such a phase is not observed.

A natural question to ask is “Where is the  $sp^2$ -liquid phase”? To answer this question it is important to consider the entropy of the various fluid phases. At low  $P$  it is clear that the linear chain structures are stabilized over  $sp^2$  or  $sp^3$  structures by entropy. At higher  $P$  the  $sp$  phase must give way to higher density phases dominated by either  $sp^2$  or  $sp^3$  bonding. The  $\sigma$  bond in the  $sp^3$  liquid allows for almost free rotations about the bond of

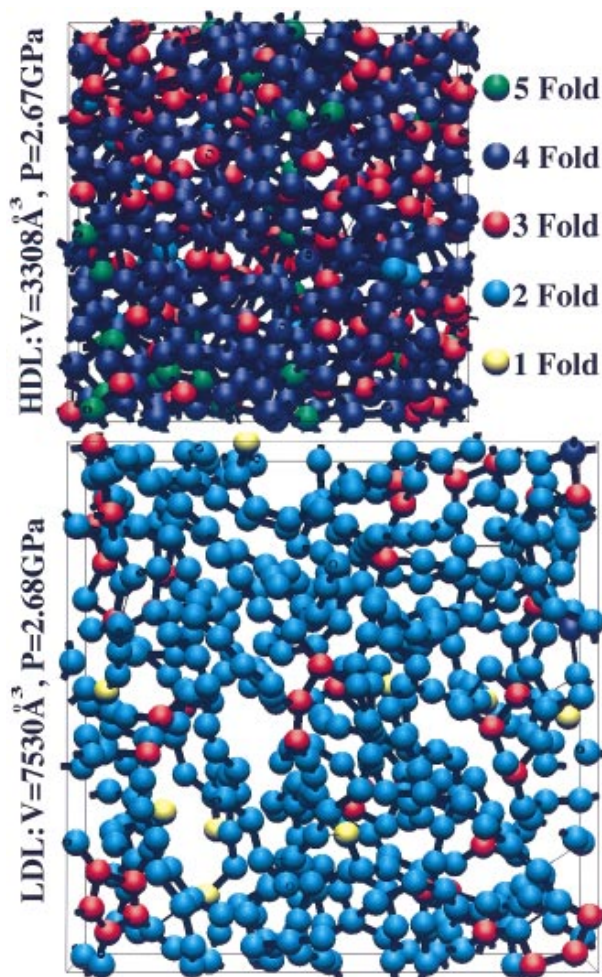


FIG. 3(color). Snapshots of a 512-particle MD configuration at 5500 K near the coexistence limits.

the local tetrahedrals, leading to many nearly equal energy conformations and high entropy. However,  $\sigma\pi$  bond in the  $sp^2$  liquid has a large rotational energy barrier, and it forces the structure to be planar, and of much lower entropy than the  $sp^3$  dominated phase. This low entropy destabilizes the  $sp^2$ -liquid phase relative to the  $sp$ - or  $sp^3$ -liquid phases. This is consistent with some unpublished work on amorphous carbon, where we found an intimate interplay between the relative stability of  $sp^2$  dominated amorphous carbon and the torsional energy about the  $sp^2$  bond. For example, without Brenner’s torsional energy term the system would quench to an almost all threefold coordinated structure, even at densities as high as diamond. The fourfold (or  $sp^3$ ) structures formed under quenching only when the torsional energy was turned on.

To further investigate the role of the torsional energy in the liquid we performed a series of calculations on the liquid state without the torsional energy term. As with quenching without torsion, the relative fraction of threefold coordinated atoms increased dramatically. Furthermore, the character of the isotherms also changed. The 6000 and 7000 K isotherms of the potential model without torsional

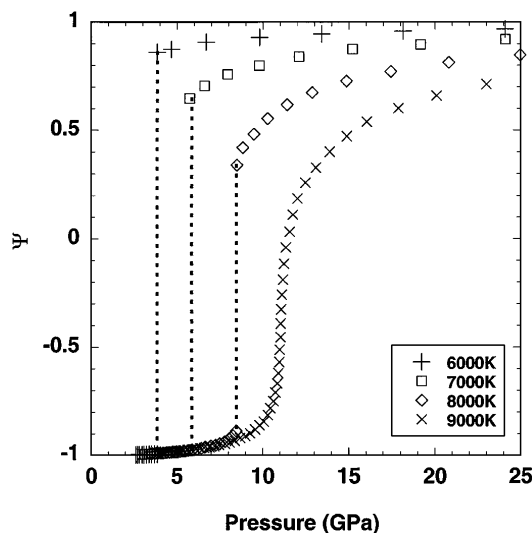


FIG. 4.  $\Psi$  vs  $P$ . At 9000 K the discontinuity vanishes.

term are shown in Fig. 1 (dotted lines) along with the set of isotherms calculated for the full potential model (solid lines). The van der Waals loop vanishes at 7000 K and is greatly reduced at 6000 K over the corresponding isotherm of the full potential model. It clearly shows the importance of the  $\sigma\pi$  bond's torsional energy.

A number of tight binding (TB) calculations have been performed on the liquid state of carbon [12,13]. At low density they predict, in agreement with this paper, twofold or chainlike structures. At higher densities, however, the TB predicts a much larger fraction of threefold coordinated atoms than predicted by this paper. This is due to the inability of the two-center approximation used in these TB calculations to model the torsional energy of rotation about the  $sp^2$  bond correctly. In fact, the twofold, threefold, and fourfold coordinated atom densities of the TB calculations are very close to our results without the torsional energy term. This may also explain why the TB results fail to predict a first order transition in the liquid region. Recently, the TB model for carbon has been extended to include three-center terms [14]. In studies of amorphous carbon [15], the use of the improved TB model is shown to greatly reduce the threefold coordinated atoms density. This new model has not yet been applied to the liquid state of carbon, but we expect that similar reductions should also occur in liquid carbon.

In both the empirical bond-order potential and the TB approximation, the van der Waals interaction has been neglected. The van der Waals attraction of about 100 K per carbon pair [16] is much smaller than the melting temperature of carbon (approximately 4500 K) and for the most part does not have a significant effect on the predicted phase diagram. An exception to this may be for the LDL phase. At low  $P$ , even at high  $T$ , the density of the LDL phase is sensitive to the long-range van der Waals forces. The inclusion of these forces should significantly increase the density of the LDL phase at a given  $P$ .

This change in the equation of state of the LDL would increase the transition pressure to the HDL phase. We are currently extending the bond-order potential model to include nonbonded interactions.

This paper strengthens the case for a first order LLPT as inferred by the experiments of Togaya. Furthermore, it lends insight into atomic structure, which has eluded experimental probing, namely, the  $sp^3$  character of the HDL and the  $sp$  character of the LDL. Although quantitative differences exist between this work and experiment, notably the low triple point pressure and the large density discontinuity, the existence and general features of LLPT in carbon have been shown. Comparison to experiment can be improved with refinements to the potential, especially with the inclusion of a van der Waals term. However, such refinements will not likely change, in a qualitative way, the findings of this paper.

The authors would like to thank M. van Thiel, G. Galli, C.-S. Yoo, H. Lorenzana, and M. Togaya for useful conversations. This work was performed under the auspices of the U.S. DOE by the Lawrence Livermore National Laboratory under Contract No. W7405-ENG-48.

- [1] O. A. Ferraz and N. H. March, *Phys. Chem. Liq.* **8**, 289 (1979).
- [2] M. van Thiel and F. H. Ree, *Phys. Rev. B* **48**, 3591 (1993); *J. Appl. Phys.* **77**, 4804 (1995).
- [3] M. Togaya, *Phys. Rev. Lett.* **79**, 2474 (1997).
- [4] K. Tsuji, *J. Noncryst. Solids* **117-118**, 27 (1990); K. Yaoita *et al.*, *ibid.* **156-158**, 157 (1993); **150**, 25 (1992); V. V. Brazhkin *et al.*, *High Press. Res.* **6**, 363 (1992); *Phys. Lett. A* **154**, 413 (1991).
- [5] O. Mishima and H. E. Stanley, *Nature (London)* **392**, 164 (1998); M.-C. Bellissent-Funel, *Europhys. Lett.* **42**, 161 (1998).
- [6] S. Harrington *et al.*, *Phys. Rev. Lett.* **78**, 2409 (1997).
- [7] D. W. Brenner, *Phys. Rev. B* **42**, 9458 (1990); **46**, 1948 (1992); D. W. Brenner *et al.*, *Thin Solid Films* **206**, 220 (1991).
- [8] H. C. Anderson *et al.*, *Report of the CECAM Workshop* (CECAM, Orsay, France, 1984).
- [9] W. G. Hoover, *Phys. Rev. A* **31**, 1695 (1985).
- [10] J. N. Glosli and F. H. Ree, *J. Chem. Phys.* **110**, 441 (1999).
- [11] F. P. Bundy, *J. Chem. Phys.* **38**, 618 (1963); **38**, 631 (1963).
- [12] J. R. Morris, C. Z. Wang, and K. M. Ho, *Phys. Rev. B* **52**, 4138 (1995).
- [13] O. Sugino, in *The Review of High Pressure Science and Technology, 1997*, edited by M. Nakahara (Japan Society of High Pressure Science and Technology, Japan, 1998), Vol. 7, p. 181.
- [14] M. S. Tang and C. Z. Wang, *Phys. Rev. B* **53**, 979 (1996).
- [15] C. Z. Wang and K. M. Ho, *Symp. Proc. Mater. Res. Soc.* **498**, 3 (1998).
- [16] W. L. Jorgensen and D. L. Severance, *J. Am. Chem. Soc.* **112**, 4768 (1990).